Low-cost and Sustainable Bioadsorbent from Banana Peel Waste for Crystal Violet Dye Removal

Salah Ud Din,^a Khairia Mohammed Al-Ahmary,^b Hamad AlMohamadi,^c Saedah R. Al-Mhyawi,^b Jawaher Saud Alrashood,^d Patrick T. Ngueagni,^{e,*} and Edwin A. Ofudje ^{fo}

A direct comparison was made between raw banana peel waste (RBPW) and acid-treated banana peel waste (ABPW), under identical conditions, for adsorption of crystal violet (CV). Sorption kinetics, isotherms, and thermodynamics were considered to reveal the underlying mechanisms. The effects of contact time, pH, initial CV concentration, temperature, and adsorbent dosage were evaluated. The sorption process obeyed a pseudo-second-order kinetic model, while the Langmuir isotherm model best explained the equilibrium data with maximum adsorption capacities. The Dubinin-Radushkevich model supported the potential of ionexchange mechanisms for the acidified sample. Adsorption was spontaneous and endothermic, as revealed by negative Gibbs free energy, positive enthalpy (+16.4 kJ/mol for RBPW and +53.5 kJ/mol for ABPW) and positive entropy (RBPW = 6.79 J/mol·K and ABPW = 14.65 J/mol·K) values. The lower ΔH for the raw peel is more consistent with physisorption, while higher ΔH of the acid-treated peel suggests stronger interactions consistent with chemisorption/ion-exchange. The FT-IR analysis confirmed that functional groups such as -OH, -COOH, C=O, C-O, and possibly aromatic moieties on banana peel waste are involved in the sorption of CV. The enhanced performance of ABPW is attributed to acid-induced surface modifications that increased porosity, making the functional groups available for sorption process.

DOI: 10.15376/biores.20.4.10640-10664

Keywords: Acid activation; Banana peel; Crystal violet; Isotherms; Kinetics

Contact information: a: Department of Chemistry, University of Azad Jammu and Kashmir Muzaffarabad, Pakistan; b: Department of Chemistry, College of Science, University of Jeddah, Jeddah, Saudi Arabia; c: Department of Chemical Engineering, Faculty of Engineering, Islamic University of Madinah, Madinah, Saudi Arabia; d: Department of Teaching and Learning, College of Education and Human Development, Princess Nourah bint Abdulrahman University, Saudi Arabia; e: Department of Inorganic Chemistry, Faculty of Science, University of Yaoundé, 812, Yaoundé, Cameroon; f: Department of Chemical Sciences, Mountain Top University, Ibafo, Ogun State, Nigeria;

INTRODUCTION

Synthetic dyes are complex organic compounds with stable structures that resist biodegradation, making them persistent environmental pollutants. It has been reported that about 12% of these dyes' annual production is released as industrial wastewater, which greatly contributes to environmental pollution (Foroutan *et al.* 2020). The release of dye components into water bodies has serious environmental and health consequences (Mahmood *et al.* 2018). Dye contamination in aquatic environments is highly visible, and it disrupts the ecosystems by hindering photosynthesis through the blocking of sunlight penetration, thus reducing oxygen levels and harming aquatic life (Baharim *et al.* 2023).

^{*} Corresponding author: patrickngueagn@gmail.com

These dyes also pose noticeable health risks, causing toxic effects such as skin irritation, carcinogenicity, allergic reactions, teratogenic effects, and potential genetic mutations, that threaten both human health and ecological systems (Patricia *et al.* 2020; El-Rayyes *et al.* 2025).

Crystal violet (CV) dye is a highly intense cationic triphenylmethane dye that is often used in pharmaceuticals, printing inks, and textiles industries (Pashaei-fakhri *et al.* 2021). The CV dye is extremely toxic; it can damage aquatic ecosystems and cause severe health related issues, among which are cardiovascular effects, respiratory problems, skin and eye irritation, and increased risks of cancer and genetic mutations (Mittal *et al.* 2021: Pashaei-fakhri *et al.* 2021). The hazardous and persistent nature of crystal violet dye has led to major research interest on the effective disposal methods for eliminating this toxic dye from wastewater.

To address this pollution challenge caused by CV and other contaminants efficiently, various techniques have engaged, and among them are chemical oxidation, coagulation, electrochemical, ozonation, nanofiltration, biological degradation, advanced oxidation processes, reverse osmosis, adsorption, and photocatalytic degradation (Ofudje et al. 2020; Wang et al. 2020; Muhammad et al. 2021; Yuan and Jiang 2021; Ngueagni et al. 2025). However, most of these conventional methods can produce secondary waste, and expensive, highlighting the need for more sustainable, and affordable solutions like adsorption (Ofudje et al. 2020). Adsorption is a very effective dye removal method, which is known for its potential for reusability, simple to operate and cost-efficiency, making it an excellent choice (Adegoke et al. 2023; Ngueagni et al. 2025). The choice of using activated carbon, which is the most common adsorbent in developing nations like Cameroon and Nigeria, is often threatened by its high cost of production (Ofudje et al. 2020). Agricultural waste-derived adsorbents are increasingly popular for wastewater treatment because of their numerous advantages, such as being efficient, cost-effective, renewable, and biodegradable (Jia et al. 2017).

Recent research has explored eco-friendly bio-adsorbents from agricultural waste, including banana trees (Abdelkhalek et al. 2022), olive stones (Abed et al. 2019), apple peels (Enniya et al. 2017), peach and apricot kernels (Rehali et al. 2021), tea waste (Liu et al. 2018), coffee grounds (Pagalan Jr et al. 2020), Kepok banana (Silviyanti et al. 2025), and corn cobs (Aljeboree et al. 2021) for effective dye and colour removal. Bananas are widely consumed worldwide, and their peels, which make up about 40% of the fruit's weight, are often disposed of as waste, causing a lot of waste management issues. However, harnessing their abundance could also make them an attractive biosorbent material for dye removal from wastewater, thus adding value to them (Akpomie and Conradie 2020). Banana peels are rich in cellulose, hemicellulose, pectin, and lignin with functional groups such as carboxyl, hydroxyl, and others which could enhance their interactions with several adsorbate, thus facilitating an effective adsorption process (Yang et al. 2019; Thomas et al. 2021). The adsorption capacity of banana peelderived adsorbents can be improved by chemical treatments such as the use of acids, bases, and salts that remove impurities and enhance properties including high porosity, and surface area (Akter et al. 2021; Channei et al. 2025). This evidence supports banana peels as promising candidates for cationic dye removal due to their natural abundance of active functional groups and modifiable structure.

Channei *et al.* (2025) reported that banana peel treated with sulfuric-acid solution resulted in a huge increase in BET surface area from just 3.2 to 339 m²/g, coupled with increased in pore volume were observed. It was reported in their work that the treatment

by an acid opened a porous network in the adsorbent by breaking the lignocellulosic structures. In a study conducted by Huang *et al.* (2024) on Cr(VI) uptake, the treatment of banana peel with 50 % H₂SO₄ at 50 °C for 24 h caused an increased its surface area from 0.036 to 0.0507 m²/g and that this improved the adsorption capacity of the adsorbent.

Many earlier works primarily focused on examining the adsorption capacity of banana peel without providing detailed mechanistic insights or comprehensive physicochemical characterizations. The present work builds upon these findings by systematically comparing raw banana peel waste (RBPW) with acidified banana peel waste (ABPW) under identical conditions. Another unique feature of this work is the integration of desorption and regeneration studies, which assessed the performance of banana peel waste across multiple adsorption—desorption cycles using acetic acid as an eluent. This sustainability aspect is often overlooked in previous banana peel studies, and it plays a critical role for practical wastewater treatment applications. The selection of acetic acid as the desorbing agent for regeneration studies was because under acidic conditions, the carboxyl groups present in lignocellulosic components of banana peel become protonated. This protonation reduces the negative surface charge that normally promotes electrostatic attraction with cationic dyes such as crystal violet. As a result, the electrostatic interactions weaken, making it easier for the bound dye molecules to be released back into solution.

This study investigated the ability of raw and acidified banana peels in adsorbing CV from wastewater. It critically examines the effects of various functions including pH, contact time, CV initial concentration, and temperature on the removal efficiency of the adsorbent. Furthermore, the research explored the thermodynamics, adsorption isotherms and kinetics involved in the process, offering a comprehensive understanding of the mechanisms behind dye removal.

MATERIALS AND METHODS

Preparation and Characterization of Acidified Adsorbent

Banana peel waste (BPW) was collected, thoroughly cleansed with deionized water, and sun-dried for seven days. The dried BPW (40 g) were subjected to acidification with 0.1 M sulfuric acid for 24 h and the content was filtered, washed using deionized water several times until neutral pH was attained, dried, and ground to powder and sieved to obtain desired particles with sizes less than 250 µm. The acidified banana peel waste (ABPW) and raw banana peel waste (RBPW), which is the untreated sample, were stored in airtight containers for further analysis.

Adsorbent Characterizations

Fourier transform infrared spectroscopy (FT-IR) (CARY630 NBY, Thermo Fisher Scientific, Waltham, MA, USA) was used for the identification of the functional groups involved in dye adsorption. Scanning electron microscopy (SEM) (Phenom ProX, USA) was used in the examination of surface morphology and porosity. Brunauer-Emmett-Teller (BET) analysis using a Quantachrome NOVA 2200C (USA) was used to determine the pore size distribution and specific surface area. The point of zero charge (pHpzc) was investigated using a Nano ZS analyzer (Malvern, UK) that assessed the surface charge behavior across pH ranges.

Crystal Violet Solution Preparation and Adsorption Study

 $1000 \, \mathrm{mg/L}$ stock solution of crystal violet (CV) was made following the dissolution of analytical-grade CV in deionized water. Different working concentrations were obtained through serial dilution. The CV solution pH was adjusted by adding either 0.1 M HCl or NaOH. For the adsorption study, 0.3 g of either ABPW or RBPW was added into 25 mL of CV solution in conical flasks and shaken at a constant temperature of 45 °C for a predetermined time. After each adsorption process, the mixtures were filtered, and the residual CV concentrations were measured using a UV-Vis spectrophotometer (Shimadzu UV-3600 UV-Vis-NIR). The CV amount sorbed at equilibrium (Q_e , mg/g) and the percentage removal (%) were estimated using Eqs. 1 and 2:

Amount adsorbed,
$$Q_e = \frac{C_o - C_e}{m}V$$
 (1)

Percentage Removal,
$$%Q_e = \frac{C_o - C_e}{C_o} x 100$$
 (2)

In these equations, C_0 is the initial CV concentration (mg/L), C_e denotes the equilibrium CV concentration (mg/L), V stands for the volume of solution (L), and m represents the mass of adsorbent used (g).

Desorption Study

To investigate the reusability of the adsorbent, desorption experiments were done using O.5M of acetic acid as the desorbing agent. The used adsorbent biomass was subjected to multiple adsorption—desorption cycles of experiments, and the percentage of CV recovered was estimated to compute the regeneration potential of the adsorbent using the equation,

$$PD(\%) = \frac{AD}{AA}X100\tag{3}$$

where AA represent the amount of CV adsorbed, DA is the amount of CV desorbed.

All experiments were performed in triplicate, and the results are represented as mean values with associated standard deviations. Error bars were included in the relevant figures.

RESULTS AND DISCUSSION

Effects of Reaction Time and CV Concentration

Crystal violet sorption onto raw and acidified banana peel waste was studied as a function of CV concentration and contact time, as presented in Figs. 1 and 2, respectively. The data indicated that the sorption process was both time- and concentration-dependent, exhibiting a rapid uptake initially, followed by a gradual approach to equilibrium. For the raw sample, at a CV 300 mg/L, the uptake capacity rose from 25.5 mg/g just after 10 min to 73.4 mg/g at 100 min. But as the contact time was extended beyond 120 min, the sorption rate slowed, and equilibrium was attained at 140 min with maximum sorption capacity of 88.5 mg/g, and beyond which no meaningful increase in the dye uptake was observed. This suggests that the available binding sites became filled with CV molecules and the system approached dynamic equilibrium (Ogundiran *et al.* 2025). The rapid uptake at the early stages could be due to the

abundance of available binding sites on the banana peel surface (El-Rayyes *et al.* 2025). For the acidified sample (Fig. 2), at 300 mg/L, the sorption capacity rose from 33.5 mg/g at 10 min to 115.5 mg/g at 120 min, and beyond which no meaningful increase in the dye uptake was observed. It was observed that the acidified banana peel consistently outperformed the raw variant at all conditions tested. For instance, the acidified peel adsorbed 96.4 mg/g of CV by 100 min, compared to 73.4 mg/g for the raw peel. The enhanced adsorption of the acidified adsorbent can be attributed to acid-induced surface modification by the removal of impurities, which increased porosity, exposed more active sites, and improved functional group affinity for CV molecules.

On the role of CV concentration, as can be seen from Figs. 1 and 2, when CV concentration was increased from 50 to 300 mg/L, the adsorption capacity also increased, reaching 19.5 mg/g at 50 mg/L and 88.5 mg/g at 300 mg/L for the raw peel and 23.4 mg/g and 115.2 mg/g in the case of the acidified peel. This increase could be a result of higher driving force for mass transfer at higher concentrations, which enables the interaction between dye molecules and the adsorbent surface to become faster. The availability of a greater number of CV molecules could promote more frequent collisions with the adsorbent, thus improving the uptake efficiency until the surface sites are fully occupied (Ogundiran et al. 2025). This consistent increase across all concentrations suggests that acid treatment enhanced the surface chemistry of the banana peel, making it more effective at capturing dye molecules. Comparable results were found by Sen et al. (2024) in the study where palm leaf sheath powder was used, showed that an increased in initial CV concentrations led to higher adsorption capacities, thereby underscoring the contribution of concentration gradient in mass transfer. Research conducted by Azhar-ul-Haq et al. (2022) employed RBPW obtained 93% CV removal and 91% desorption efficiency, with adsorption equilibrium reached within 10 min, highlighting rapid kinetics even with untreated biomass.

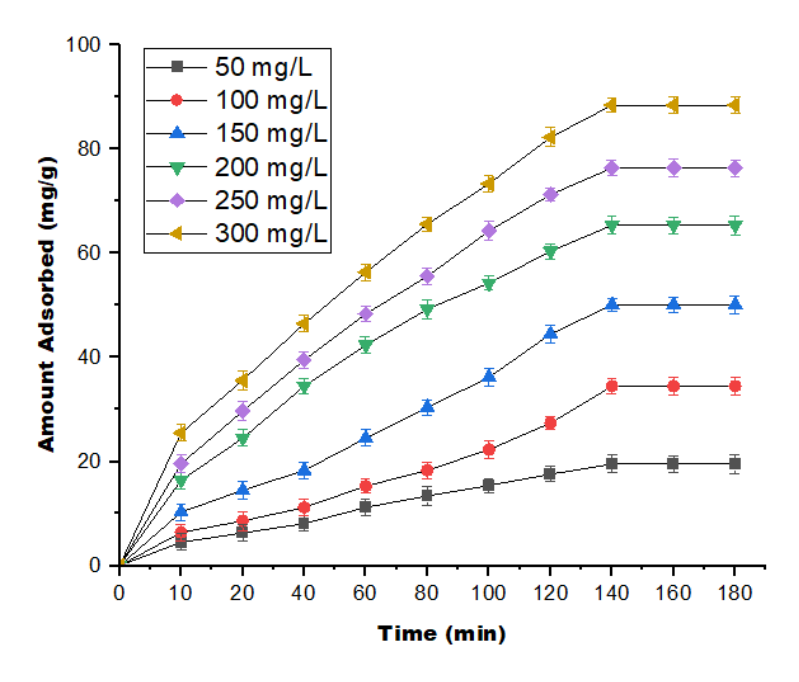


Fig. 1. Graphs of contact time and CV concentrations for the sorption by RBPW

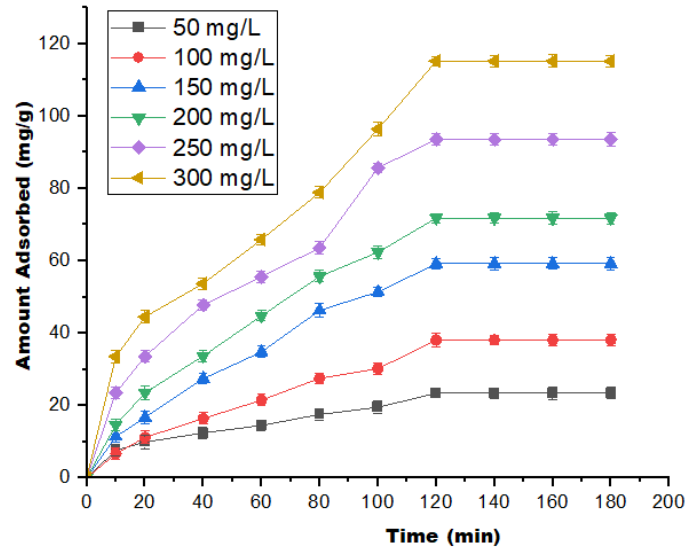


Fig. 2. Graphs of contact time and CV concentrations for the sorption by ABPW

Effect of Banana Peel Waste Dosage

The influence of banana peel dosage on the removal of CV dye was evaluated using both raw banana peel waste (RBPW) and acidified banana peel waste (ABPW), with dosages ranging from 0.1 g to 0.4 g as depicted in Fig. 3.

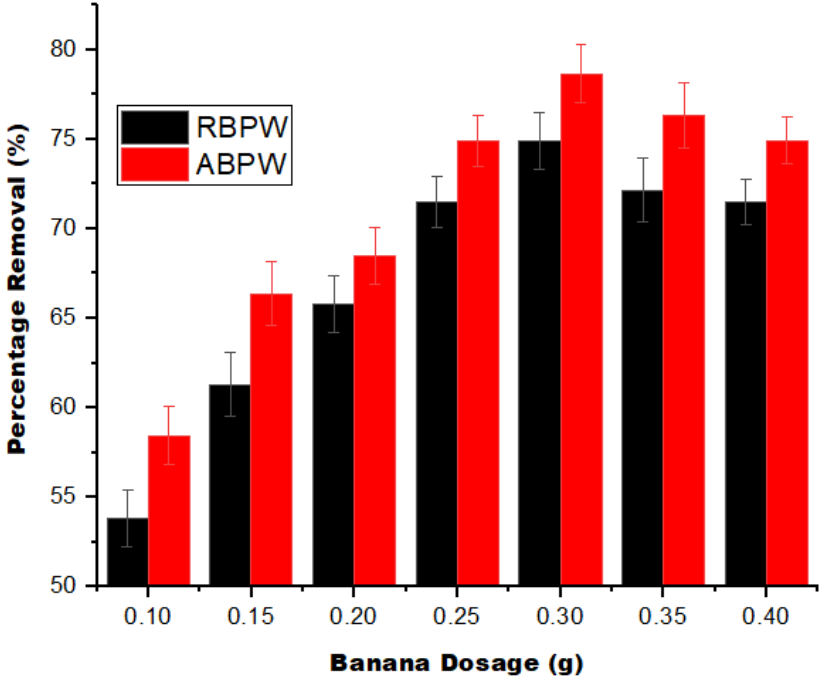


Fig. 3. Graph of dosage effects on the uptake of CV by RBPW and ABPW

For RBPW, adsorption percentage rose from 53.8% at 0.1 g to a peak of 74.9% at 0.3 g and above this point, a marginal decrease was noted, with values of about 71.5% recorded at 0.4 g. Similarly, ABPW demonstrated improved performance across all dosages, achieving a maximum adsorption of 78.7% at 0.3 g, then slightly decreasing to

74.9% at 0.4 g. In both cases, the sorption percentage increased with dosage up to 0.3 g, after which a slight decline was observed. While this trend is often attributed to overlapping and aggregation of active sites at higher biomass concentrations (Shridhar and Sanjaykumar 2022; Ogundiran *et al.* 2025), another important factor is the physical nature of banana peel material. Being pulpy and crumbly, higher dosages increase the likelihood of generating very fine particles that disperse in solution. These fines can adsorb dye molecules but may not be fully retained during filtration, causing an underestimation of adsorption performance.

In a study by Baharim *et al.* (2023), acidic post-treatment of banana pseudo-stem biochar showed enhanced CV uptake up to an optimal dose after which additional dose yielded negligible benefits due to saturation effects. Furthermore, Shridhar and Sanjaykumar (2022) observed that adsorbent obtained from banana stems demonstrated exceptionally high CV adsorption capacities (up to 208 mg/g), indicating that the chemical treatment of banana-based biomass enhanced dye uptake beyond quantities observed here and in RBPW.

Effect of pH on the Adsorption of Crystal Violet

Solution pH plays a vital role in the uptake of CV dye onto banana peel-based adsorbents, as it influences both the adsorbent's surface charge and the dye molecules' ionization state. In this study, the adsorption capacities of RBPW and ABPW were evaluated over a pH range of 2.0 to 6.0, as shown in Fig. 4. For both adsorbents, the percentage removal rose with rising pH from 2.0 to 4.5, reaching a maximum at pH 4.5 for ABPW (80.5%) and pH 5.0 for RBPW (74.83%). At lower pH values, protonation of functional groups on the banana peel surface could result in an overall positive surface charge, which creates electrostatic repulsion between the cationic CV molecules and the surface of the adsorbent. This could lead to lower adsorption capacities at acidic pH conditions, as seen in this current study with values of 49.6% for RBPW and 53.7% for ABPW at pH 2.0.

As the pH rises, adsorbents surface becomes less protonated and more negatively charged, enhancing electrostatic attraction between the CV cations and the adsorbent surface. This leads to increased dye uptake. The higher performance of ABPW across all pH values can be attributed to acid treatment, which enhances surface area, introduces more acidic functional groups, and increases the number of negative sites available for cationic dye binding. The point of zero charge (pHzPC) were found to be 4.7 in the raw material and 4.1 in the acidified form. These values indicate the pH at which the surface of the adsorbent carries no net charge. At pH values less than the pHzPC, the surface will be positively charged, but at pH values above it, the surface is negatively charged. Since CV is a cationic dye, it's uptake is generally favored on negatively charged surfaces due to electrostatic attraction. For the raw adsorbent, maximum adsorption was observed at pH 4.5, which is slightly below its pHzPC of 4.75. At this pH, the surface of the adsorbent is expected to be mildly positively charged, which would typically repel the CV molecules which are positively charged. However, the high adsorption observed suggests that mechanisms other than electrostatic attraction, such as Van der Waals forces, $\pi - \pi$ interactions or hydrogen bonding between the aromatic rings of the dye and the lignocellulosic components of the bark, likely played a significant role in dye uptake. This implies that despite mild electrostatic repulsion, other physicochemical interactions were strong enough to drive substantial adsorption at this pH.

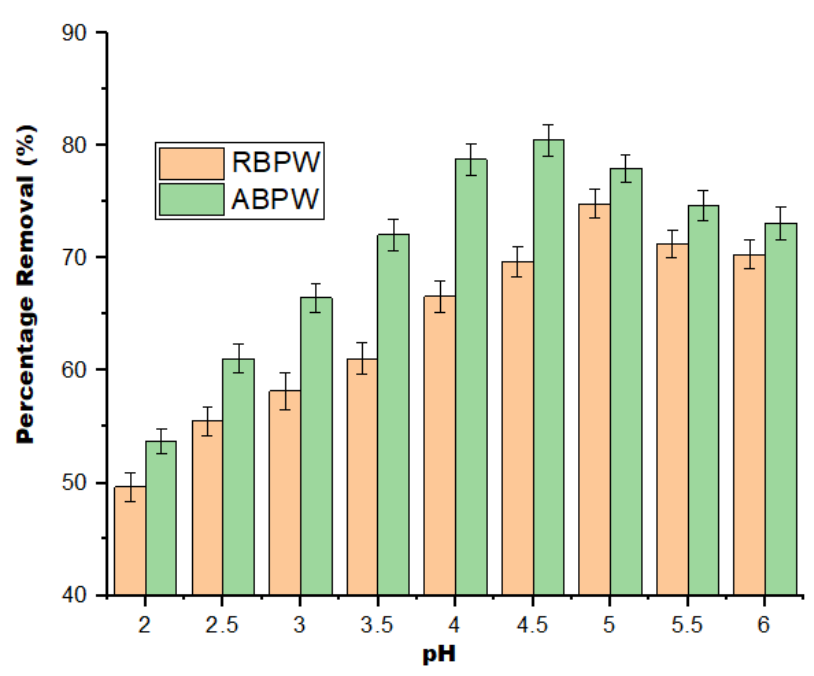


Fig. 4. Graphs of effect of pH on the uptake of CV by RBPW and RBPW

In contrast, the acidified sample showed maximum adsorption at pH 5.0, which is above its pHzPC of 4.14. This implies that the surface was negatively charged at the optimum pH, favoring electrostatic attraction with the cationic dye. The acid treatment likely enhanced the surface acidity and shifted the pHzPC to a lower value. This modification improved the surface's affinity for positively charged species at slightly acidic to neutral pH levels, thereby increasing the adsorption efficiency. However, beyond the optimum pH, a gradual decline in adsorption percentage was observed. For ABPW, the percentage dropped from 80.5% at pH 4.5 to 73.1% at pH 6.0, and for RBPW, from 74.8% at pH 5.0 to 70.3% at pH 6.0. The decline may result from saturation of binding sites and competition with OH⁻ ions at higher pH, limiting dye uptake. The observed trends are consistent with prior studies. For example, Azhar-ul-Haq *et al.* (2024), reported optimal CV binding by banana peel powder at pH near neutral, achieving ~93% removal in a rapid 10 min contact time confirming that CV adsorption is favored in mild-to-moderately acidic conditions.

The FT-IR analysis indicated shifts in –OH and C=O stretching bands after the sorption, suggesting the likely involvement of hydrogen bonding between CV molecules and surface hydroxyl/carbonyl groups (Ahmed *et al.* 2024; Cao *et al.* 2024). In addition, the shifts noticed in aromatic C=C bands support the occurrence of π – π stacking interactions between the lignin/phenolic structures of banana peel and the aromatic rings of CV (Guo *et al.* 2023; Ahmed *et al.* 2024). These extra interactions complement electrostatic attraction, explaining the relatively high adsorption even at pH values close to the pHpzc where electrostatic effects alone would be unfavorable. For instance, Guo *et al.* (2023) noted that the combining effect of π – π and hydrogen bonding interactions can double adsorption energy for dyes on biochar, when compared to electrostatic-only mechanisms. A study by Cao *et al.* (2024) using DES-functionalized ZIF-8/carbon adsorbents reported enhanced adsorption of mephedrone from pH 5 to 11, which was concluded to have been driven by the synergy of π – π stacking and hydrogen bonding.

Another feature that can influence the pH is the charge characteristics of the dye, as crystal violet contains one quaternary amine group and two tertiary amine groups. The quaternary amine can remain positively charged at all pH values, whereas the tertiary amines are protonated at very low pH in the range of 1 to 2 but progressively deprotonate as pH increases (Huang *et al.* 2023). Thus, at highly acidic pH, the molecules of CV carry multiple positive charges, which, together with the protonated adsorbent surface, creates strong electrostatic repulsion and results in low dye uptake. But as the pH rose, the tertiary amines lose protons, reducing the dye's net positive charge and decreasing repulsion (Huang *et al.* 2023). Within this range, electrostatic attraction between the negatively charged adsorbent sites and remaining positively charged quaternary group, along with hydrogen bonding and π - π interactions, become more dominant, leading to enhanced sorption.

Effect of Temperature on CV Adsorption by RBPW and ABPW

In this study, the sorption percentage of CV onto RBPW and ABPW was evaluated from 25 to 55 °C, as shown in Fig. 5. For both adsorbents, an elevated temperature caused an improved adsorption performance. RBPW's adsorption percentage rose from 51.1% at 25 °C to 76.1% at 45 °C, maintaining this peak value at 50 and 55 °C. Similarly, ABPW showed a higher increase, from 58.7% at 25 °C to a maximum of 84.6% at 50 and 55 °C. The adsorption efficiency increasing with rising temperature is an indication that the overall process of CV uptake by banana peel waste is endothermic in nature. This enhancement can be attributed to stronger interactions with surface functional groups and mobility of dye molecules at elevated temperatures. This trend aligns with findings from Gemici (2023), who investigated CV adsorption onto sulfuricacid-treated chestnut shell and observed an increased in adsorption capacities with rising temperatures (25 to 50 °C).

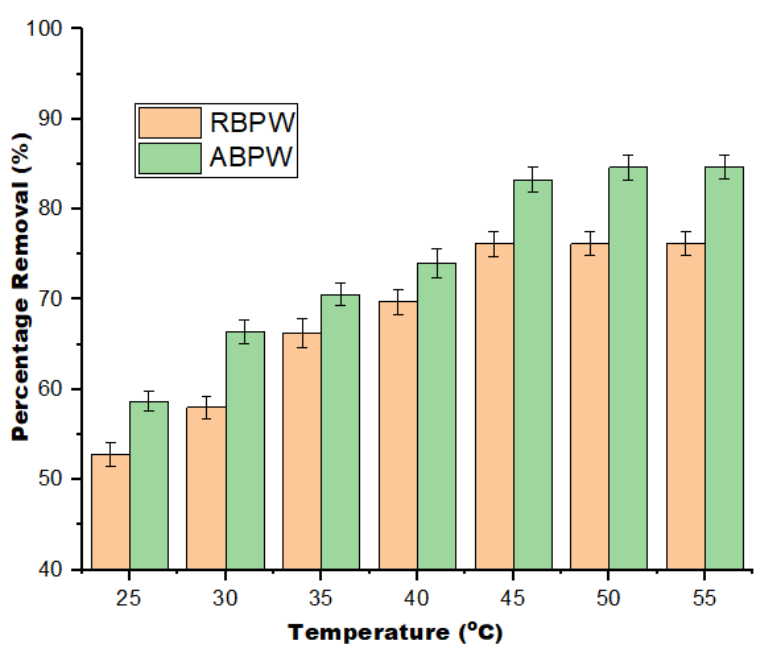


Fig. 5. Graphs of effect of temperature on the uptake of CV by RBPW and ABPW

Kinetic Modeling of CV Adsorption onto RBPW and ABPW

The pseudo-first-order model (Eq. 4), pseudo-second-order model (Eq. 5), and intraparticle diffusion model (Eq. 6) were used to describe the kinetic behavior of the sorption of CV by RBPW and ABPW (Parlayıcı and Baran 2025):

$$\log(Q_e - Q_t) = \log Q_e - \frac{k_1}{2.303}t \tag{4}$$

$$t/Q_{t} = 1/k_{2}Q_{t} + t/Q_{e}$$
(5)

$$Q_t = k_p t^{1/2} + C_i \tag{6}$$

Here k_1 stands for pseudo-first-order rate constant (min⁻¹), k_2 denotes pseudo-second-order rate constant (g/mg·min), k_p stands for intra-particle diffusion rate constant (mg/g/min^{1/2}), C_i denotes the boundary layer thickness, Q_t and Q_e have been defined previously, and t is time (min). The suitability of the most fit was determined by root mean square error as listed in Eq. 7 below (Sahmoune *et al.* 2024),

$$RMSE = \sqrt{\frac{\sum_{i}^{N} (Q_{(exp)} - Q_{(cal)})^{2}}{N}}$$
(7)

where N expresses the data points number, while the remaining parameters have been defined previously.

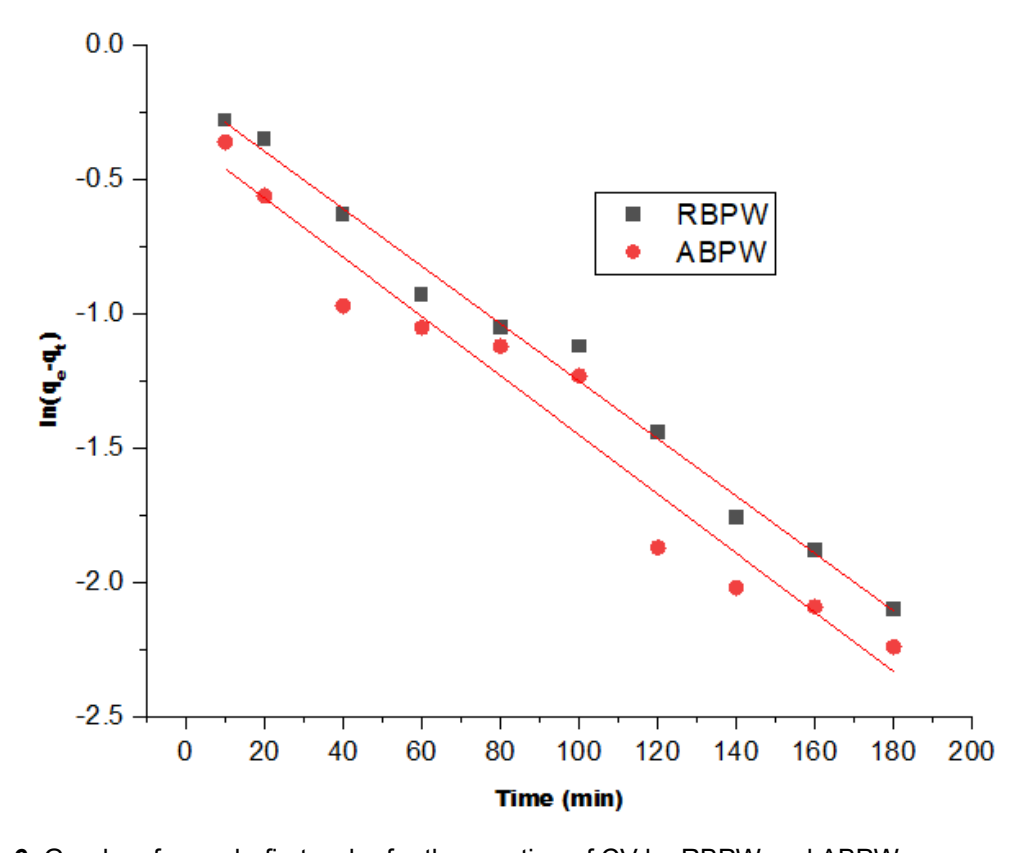


Fig. 6. Graphs of pseudo-first-order for the sorption of CV by RBPW and ABPW

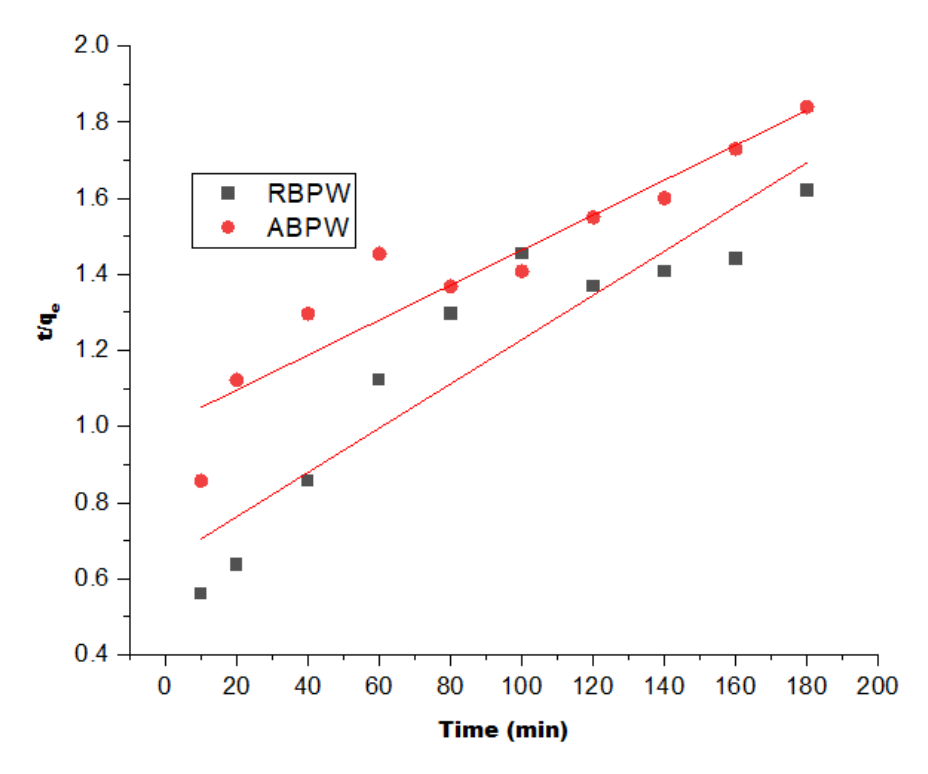


Fig. 7. Graphs of pseudo-second-order for the sorption of CV by RBPW and ABPW

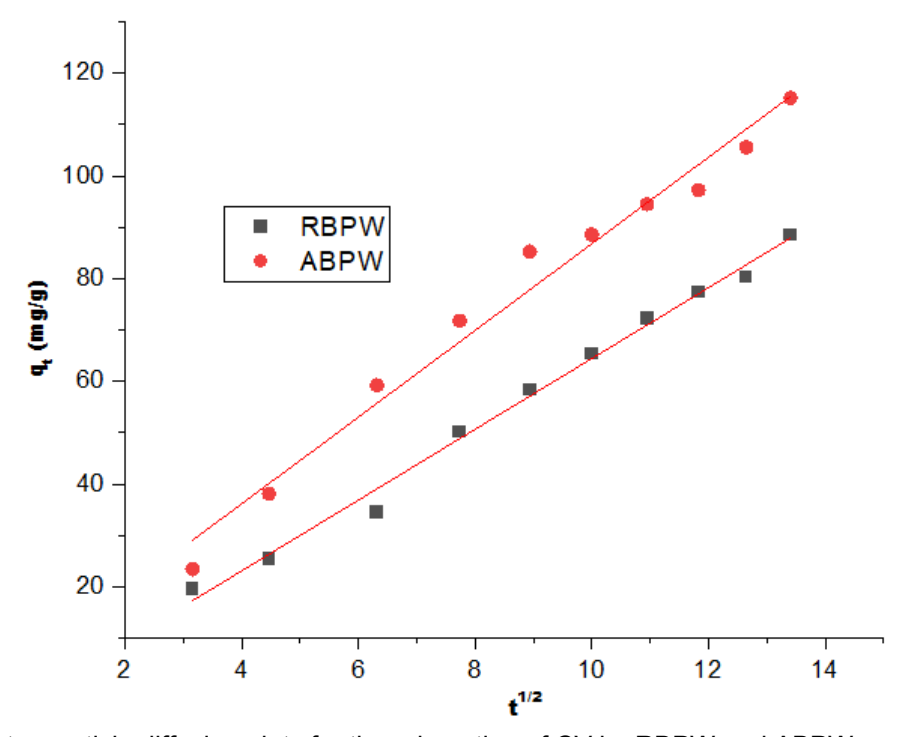


Fig. 8. Intra-particle diffusion plots for the adsorption of CV by RBPW and ABPW

The data obtained from Figs. 6, 7, and 8 for the kinetics study are listed in Table 1. The pseudo-first-order model, reflecting diffusion-limited adsorption, fitted the RBPW and ABPW data well in terms of R^2 (0.994–0.998), but it consistently underestimated equilibrium adsorption capacity (Q_e cal). In contrast, the pseudo-second-order model,

provided calculated Q_e values closely matching with experimental ones, with high coefficients of determination ($R^2 \approx 0.966-0.998$) and very low SSE percentages (< 0.05). These results clearly indicate that the adsorption process was well fitted by both the pseudo-first-order and pseudo-first-order models. Research on palm leaf sheath powder by Sen *et al.* (2024) confirmed pseudo-second-order as the most appropriate kinetic model for CV adsorption.

The intraparticle diffusion model revealed high R^2 values (0.975 to 0.996) for both raw and acidified adsorbents, but the graph did not pass through the origin, indicating that intraparticle diffusion was substantial but not the sole rate-limiting process. Constant C_i values ranging from ~ 0.099 to ~ 2.19 further confirm that boundary-layer diffusion influences adsorption. Although both the pseudo-first-order and pseudo-second-order models showed a good fit for CV adsorption, this alone does not conclusively indicate a specific mechanism. However, insights from the intraparticle diffusion model suggest that the overall adsorption is likely diffusion-controlled, particularly within a network of fine pores in an adsorption mechanism that aligns well with the porous structure of adsorbents derived from biomass such as banana peel waste (Hubbe *et al.* 2019).

Table 1. Kinetic Parameters of CV Adsorption by RBPW and ABPW

	RBPW										
	First Order			Second Order				Intra Particle Diffusion			
Q _e (exp)	Q _e (cal)	k 1	R ²	% SSE	Q _e (cal)	k 2	R ²	% SSE	k p	Ci	R ²
19.500	20.150	0.014	0.995	0.010	21.850	0.018	0.967	0.036	2.670	0.099	0.975
34.500	35.650	0.016	0.996	0.010	35.650	0.022	0.966	0.010	4.060	0.105	0.995
50.100	49.510	0.017	0.998	0.004	48.510	0.042	0.948	0.010	7.807	0.277	0.988
65.400	64.307	0.019	0.996	0.005	60.307	0.068	0.955	0.023	9.857	0.591	0.995
76.400	77.020	0.021	0.997	0.002	73.820	0.072	0.956	0.010	11.400	1.326	0.976
88.500	87.877	0.026	0.994	0.002	85.877	0.091	0.963	0.009	14.223	2.189	0.986
ABPW											
	First Order			Second Order				Intra Particle Diffusion			
Q _e (exp)	Q _e (cal)	<i>k</i> ₁	R ²	% SSE	Q _e (cal)	k ₂	R ²	% SSE	k _p	Ci	R ²
23.400	22.960	0.297	0.933	0.006	23.060	0.011	0.998	0.004	5.260	0.119	0.992
38.100	44.430	0.388	0.946	0.050	43.440	0.053	0.988	0.042	7.001	0.336	0.995
59.200	61.950	0.415	0.894	0.014	63.760	0.353	0.990	0.023	9.790	0.531	0.993
71.800	74.820	0.553	0.885	0.013	73.480	0.674	0.987	0.007	12.400	0.649	0.985
93.600	97.100	0.793	0.936	0.011	91.230	1.026	0.998	0.008	18.700	0.700	0.993
115.00	121.050	0.888	0.927	0.015	113.750	1.680	0.957	0.004	22.500	0.900	0.996

Isotherms of CV Adsorption onto RBPW and ABPW

Three isotherm models of Langmuir, Freundlich, and Dubinin–Radushkevich (D–R) were used to explain the relationship between the adsorbent and the adsorbate at equilibrium, as represented in Eqs. 8, 9, and 10 below (Dada *et al.* 2012; Ofudje *et al.* 2024; Sen *et al.* 2024; Channei *et al.* 2025; Ogundiran *et al.* 2025):

$$\frac{C_e}{q_e} = \frac{1}{bq_m} + \frac{C_e}{q_m} \tag{8}$$

$$Inq_e = InK_F + \frac{1}{n}C_e \tag{9}$$

$$Inq_e = Inq_m - \beta \Sigma^2 \tag{10}$$

The maximum adsorption capacity is denoted as Q_{max} (mg/g), b depicts the Langmuir constant in L/mg, Freundlich constant is given as K_F (mg/g), and n represents the adsorption intensity, which determines the favorability of adsorption process or otherwise. From D-R, q_e and q_m have been defined previously, ϵ is the Polanyi potential. The separation factor (R_L) from the Langmuir isotherm that determines the favorability of adsorption can represented as (Ofudje *et al.* 2024):

$$R_{L} = \frac{1}{(1+bC_{o})} \tag{11}$$

When $0 < R_L < 1$, the adsorption is said to be favorable, but when $R_L > 1$, it's unfavorable adsorption, with $R_L = 1$, the process is linear adsorption, and irreversible adsorption if $R_L = 0$. The data obtained from Figs. 9, 10, and 11 for the isotherms study are listed in Table 2. The sorption equilibrium data as obtained for both RBPW and ABPW fit well to the Langmuir isotherm model. RBPW had a maximum adsorption capacity (Q_{max}) of 93.15 mg/g ($R^2 = 0.975$), while ABPW shows a notably higher Q_{max} of 122.53 mg/g ($R^2 = 0.988$). Additionally, the Langmuir separation factor (R_1) values of 0.524 for RBPW and a significantly lower 0.041 for ABPW confirm favorable adsorption, with ABPW presenting a highly favorable process. This observation is consistent with recent studies where acid or phosphoric acid treatment of banana peel and similar biomass adsorbents increased Q_{max} and reduced R_{l} , indicative of improved monolayer dye uptake (Channei et al. 2025). When the Freundlich isotherm was assessed, it equally presented a good fit, especially for ABPW (R² = 0.995). The Freundlich constant K_F for ABPW (76.41) exceeded that of RBPW (64.61), signifying higher adsorption intensity, while the 1/n values (0.630 for RBPW; 0.231 for ABPW) imply both materials had favorable adsorption affinity, though ABPW displayed a much stronger adsorption intensity towards the adsorbent (Palle et al. 2022). Such dual fitting to Langmuir and Freundlich models is commonly observed in chemically modified bioadsorbents, especially where surface treatment enhances dye-adsorbent interactions.

The Langmuir model fit suggests that monolayer adsorption of crystal violet occurs on a relatively homogeneous surface of banana peel-based adsorbents, particularly after acid modification, which increases uniformity of active sites. On the other hand, the good fit of the Freundlich model indicates surface heterogeneity and the possibility of multilayer adsorption, reflecting the complex structure of lignocellulosic biomass that contains different types of functional groups (–OH, –COOH, C=O, aromatic rings). The dual fitting therefore implies that while adsorption is predominantly monolayer

(supported by high $Q_{\rm max}$ values), additional multilayer interactions may also occur, especially at higher dye concentrations, likely due to hydrogen bonding and π - π stacking between dye molecules and the biomass surface. This complementary behavior of both models has been observed in other dye-biomass systems and highlights that the adsorption process is controlled by a combination of homogeneous monolayer binding sites and heterogeneous multilayer sorption sites. Jahin *et al.* (2024) reported dual fitting as evidence of both homogeneous binding sites and multilayer or heterogeneous adsorption phenomena.

The Dubinin–Radushkevich (D–R) isotherm further elucidates the adsorption mechanism by estimating the mean free energy E and Polanyi potential constant, ϵ as presented in Eqs. 12 and 13. respectively (Dada *et al.* 2012; Ofudje *et al.* 2024),

$$E = \frac{1}{\sqrt{2\beta}}$$

$$\Sigma = RTIn(1 + \frac{1}{C_e})$$
(12)

where Σ is defined as the Polanyi potential constant, the mean free energy of adsorption is presented as E (kJ/mol). An insight from the value of E could provide information about the adsorption mechanism; with E found between 8 and 16 kJ/mol, to be chemical or ion exchange, but E < 8 kJ/mol, is said to be physical adsorption process (Dada et~al. 2012; Ofudje et~al. 2024). For RBPW, E is 4.34 kJ/mol, indicating physical adsorption via Van der Waals forces, but in contrast, ABPW's E value of 10.8 kJ/mol bridges the range into ion-exchange or chemical adsorption territory. Literature report by Ofudje et~al. (2024) corroborates this, with study on unmodified and modified sugarcane peel biomass (including banana peel) showing similar E values of 4.642 kJ/mol for unmodified and 31.0 kJ/mol for modified sample, suggesting physisorption and chemisorption mechanism in the uptake of methylene blue.

Table 3 presents a comparative analysis of different adsorbents based on their maximum adsorption capacities for CV dye removal, highlighting the performance of banana peel-based adsorbents. Among all materials studied, acidified banana peel waste from this study exhibited the high adsorption capacity at 122.5 mg/g, surpassing both natural and chemically modified adsorbents reported in the literature. Raw banana peel waste also demonstrated a strong performance with an adsorption capacity of 93.2 mg/g, indicating the intrinsic potential of banana peel as an effective biosorbent. Comparatively, other natural biomass adsorbents such as banana pseudo stem (48.2) mg/g), Prunus spinosa (53.2 mg/g), and Raphanus caudatus biomass (48.7 mg/g) showed moderate adsorption capacities. While chemical modifications such as polyacrylamide grafting enhanced the performance of kiwi fruit peel powder (69.9 mg/g) and Actinidia deliciosa peels (75.2 mg/g), they still fell short of the performance exhibited by ABPW. Notably, even advanced materials like Fe₃O₄-decorated bacteria (114.6 mg/g) were outperformed by ABPW. These findings underscore the effectiveness of banana peel waste, particularly when acidified, as a low-cost, high-efficient adsorbent for dye removal, reinforcing its potential for use in wastewater treatment applications.

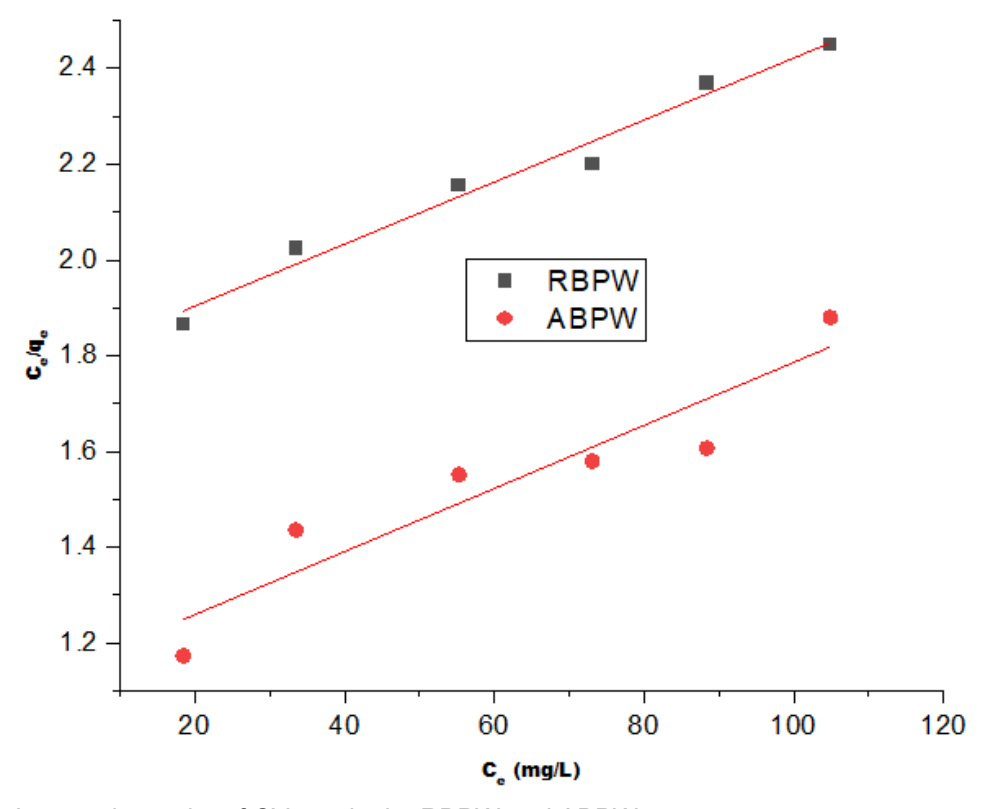


Fig. 9. Langmuir graphs of CV uptake by RBPW and ABPW

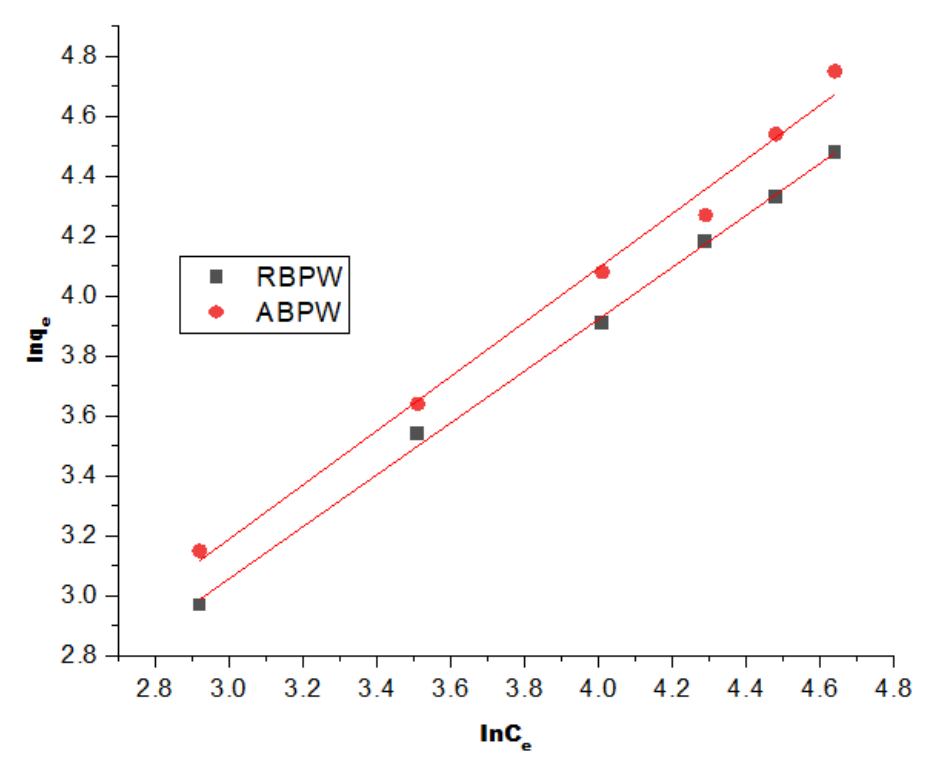


Fig. 10. Freundlich graphs of CV uptake by RBPW and ABPW

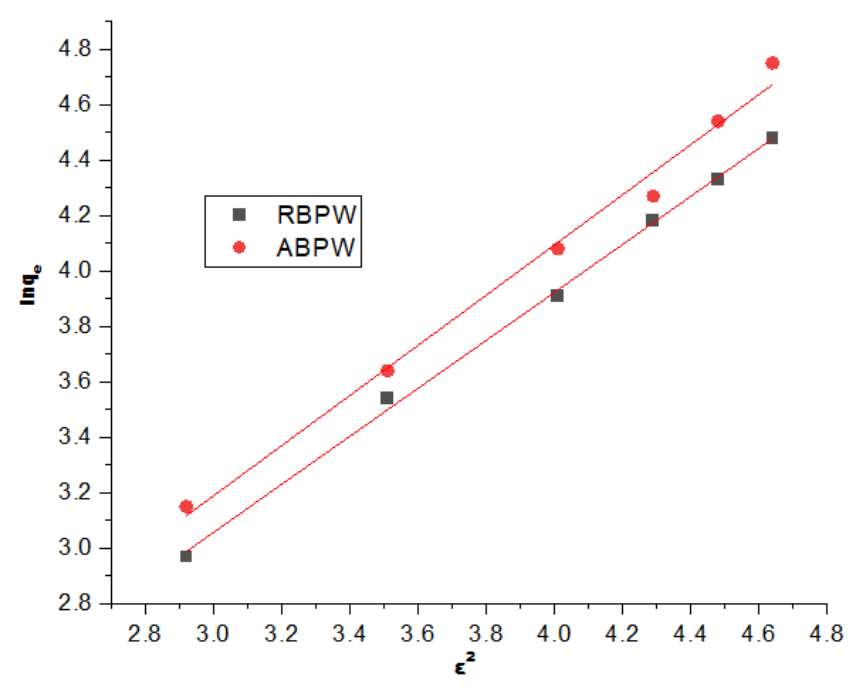


Fig. 11. Dubinin-Radushkevich graphs of CV uptake by RBPW and ABPW

Table 2. Isotherms Parameters of CV Adsorption onto RBPW and ABPW

	Parameters	RBPW	ABPW
	Q _{max} (mg/g)	93.15	122.53
Langmuir	RL	0.524	0.041
	R^2	0.975	0.988
	<i>K</i> _F (mg/g)(mg/L) ^{-1/2}	64.61	76.41
Freundlich	1/n	0.630	0.231
	R^2	0.963	0.995
	Q₅ (mg/g)	77.47	96.47
Dubinin-Radushkevich	E (kJ/mol)	4.34	10.82
	R^2	0.985	0.971

Table 3. Comparative of Different Adsorbents Capacities with Banana Peel Waste for CV Adsorption

Adsorbents	Q _{max}	References
	(mg/g)	
Banana Pseudo Stem	48.2	Baharim <i>et al</i> . (2023)
Prunus spinosa	53.19	Onuk and Isik (2025)
Raphanus caudatus biomass	48.70	Naseem <i>et al.</i> (2023)
Polyacrylamide-grafted kiwi fruit peel powder	69.93	Ahmad, and Ansari (2020)
Activated rice husk	62.85	Homagai <i>et al.</i> (2022)
Fe₃O₄ decorated bacteria	114.6	Cheng <i>et al</i> . (2023)
Polyacrylamide-grafted Actinidia deliciosa peels powder	75.19	Ahmad and Ansari (2020)
RBPW	93.2	This study
ABPW	122.5	This study

Thermodynamics of Crystal Violet Adsorption

Thermodynamic information was obtained from free energy change (ΔG°), enthalpy change (ΔH°), and entropy change (ΔS°) using equations 14, 15, and 16 (Edet and Ifelebuegu 2020; Ofudje *et al.* 2024),

$$K_d = {^q_e}/{C_e} \tag{14}$$

$$\ln K_d = \frac{\Delta S^o}{R} - \frac{\Delta H^o}{RT} \tag{15}$$

$$\Delta G^o = RTInK_d \tag{16}$$

where T is temperature in Kelvin unit (K) and the universal gas constant in 8.304 J $\text{mol}^{-1}\text{K}^{-1}$ is denoted by R. Figure 12 was used to compute the values of parameters listed in Table 4. The Gibbs free energy gave negative values (ΔG°) across all temperatures for both RBPW (-0.25 to -1.25 kJ/mol), and ABPW (-0.43 to -2.03 kJ/mol) is an indication that CV adsorption is spontaneous (Azhar-ul-Haq *et al.* 2022). The trend toward more negative ΔG° as temperature increases underscores the favorability of adsorption at higher temperatures (Edet and Ifelebuegu 2020). The positive enthalpy changes (+16.35 kJ/mol for RBPW and +53.46 kJ/mol for ABPW) indicate the endothermic nature of the adsorption (Dada *et al.* 2012). These findings are consistent with the outcome of the findings reported by Azhar-ul-Haq *et al.* (2022) where the uptake of CV by banana peel–based adsorbent gave ΔG° to be negative, and ΔH° as positive, indicating spontaneous, endothermic adsorption. Adsorption enthalpies smaller than 40 kJ·mol⁻¹ are classified as physisorption, whereas those with values greater than this are said to be an indicative of chemisorption (Girish 2025). In this study, the ΔH values from RBPW and ABPW suggest physisorption and chemisorption/ion-exchange respectively.

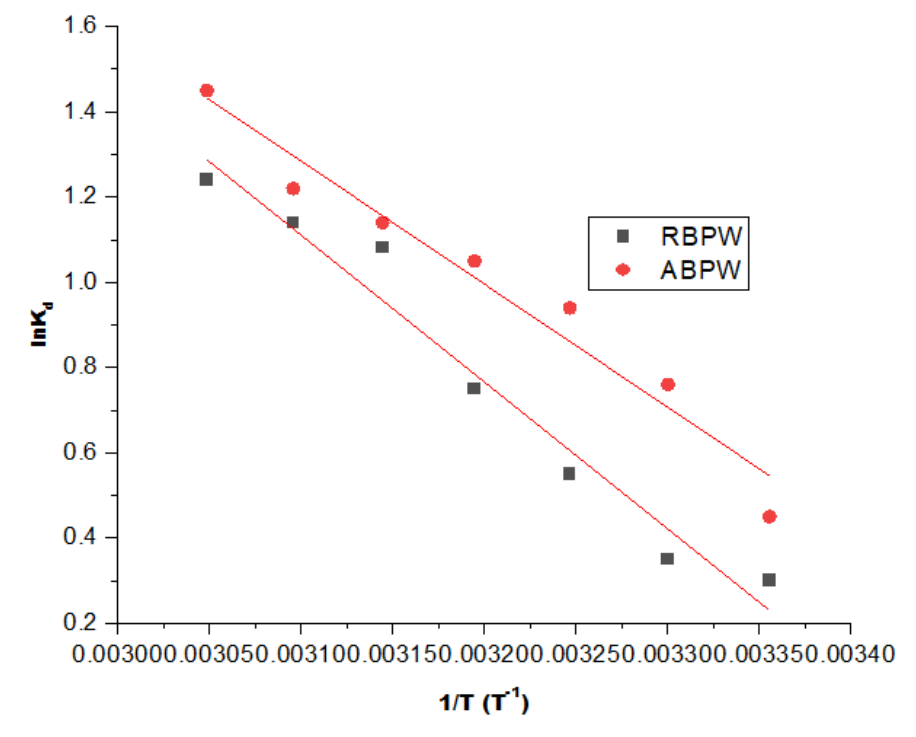


Fig. 12. Thermodynamic graphs of CV uptake by RBPW and ABPW

Literature supports this with Gemici *et al.* (2023) reporting a similar trend of endothermic adsorption when studying chemically modified lignocellulosic wastes for CV removal. The entropy change analysis showed that adsorption of CV onto both raw and acidified banana peel waste was accompanied by an increase in randomness, which becomes more pronounced with acid treatment (RBPW = 6.79 J/mol·K and ABPW = 14.65 J/mol·K). Acidification possibly removed surface impurities or modified surface charges, leading to better dye dispersion and less structured adsorption layers. This enhanced entropy effect contributes to the greater spontaneity and thermodynamic favorability of dye removal using ABPW compared to RBPW.

Table 4. Values of Thermodynamics Constants for the Sorption of CV by Raw and Acidified Banana Peel Waste

		RBPW		ABPW			
<i>T</i> (K)	ΔG (kJ/mol)	Δ <i>H</i> (kJ/mol)	ΔS (J/mol·K)	ΔG (kJ/mol)	Δ <i>H</i> (kJ/mol)	ΔS (J/mol·K)	
298	-0.25			-0.43			
303	-0.44			-0.74			
308	-0.68			-0.86			
313	-0.85	16.35	6.79	-1.04	53.46	14.65	
318	-1.05			-1.49			
323	-1.11			-1.75			
328	-1.25			-2.03			

Fourier Transform Infra-Red Analysis

The Fourier transform infrared (FTIR) spectra of banana peel waste before and after sorption of CV is provided in Fig. 13, which gave valuable insights into the functional groups involved in the sorption process and confirm the interaction between the dye molecules and the adsorbent surface. Before sorption, a broad, strong peak indicating hydroxyl groups (-OH), typical of cellulose, hemicellulose, and lignin in banana peels was seen at 3350 to 3565 cm⁻¹ (Popoola et al. 2024). After sorption, this peak shifted to 3325 to 3478 cm⁻¹ and became reduced in intensity, suggesting that -OH groups are likely involved in hydrogen bonding or electrostatic interactions with CV dye molecules. The peak found around 2965 cm⁻¹, which is attributed to C-H, is present in both spectra but showed a minor shift and intensity change, indicating that aliphatic chains may experience minor interactions during dye binding. The band near 1730 cm⁻¹, which is assigned to C=O stretching of carboxylic acids or esters in the sample before adsorption, was shifted to 1745 cm⁻¹ in the sample after adsorption of CV (Popoola et al. 2024). The prominent bands at 1685 cm⁻¹ and 1466 cm⁻¹ indicating the presence of aromatic C=C stretch before adsorption also were shifted to 1674 cm⁻¹ and 1457 cm⁻¹ after the adsorption process. These clear shifts and reduced intensity after sorption are likely indicative of the involvement of aromatic rings group, supporting π – π interactions and/or electrostatic attraction between CV and the banana peel surface. The peak seen at 1150 cm⁻¹ in the banana peel before CV adsorption was reduced to 1143 cm⁻¹, indicating the involvement of C-O stretch.

The –OH stretching band, which shifted from 3350–3565 cm⁻¹ to 3325–3478 cm⁻¹, the C=O band that moved from 1730 cm⁻¹ to 1745 cm⁻¹, and the aromatic C=C bands that shifted from 1685 and 1466 cm⁻¹ to 1674 and 1457 cm⁻¹ suggest possible

involvement of hydroxyl, carbonyl, and aromatic groups in the adsorption of CV molecules.

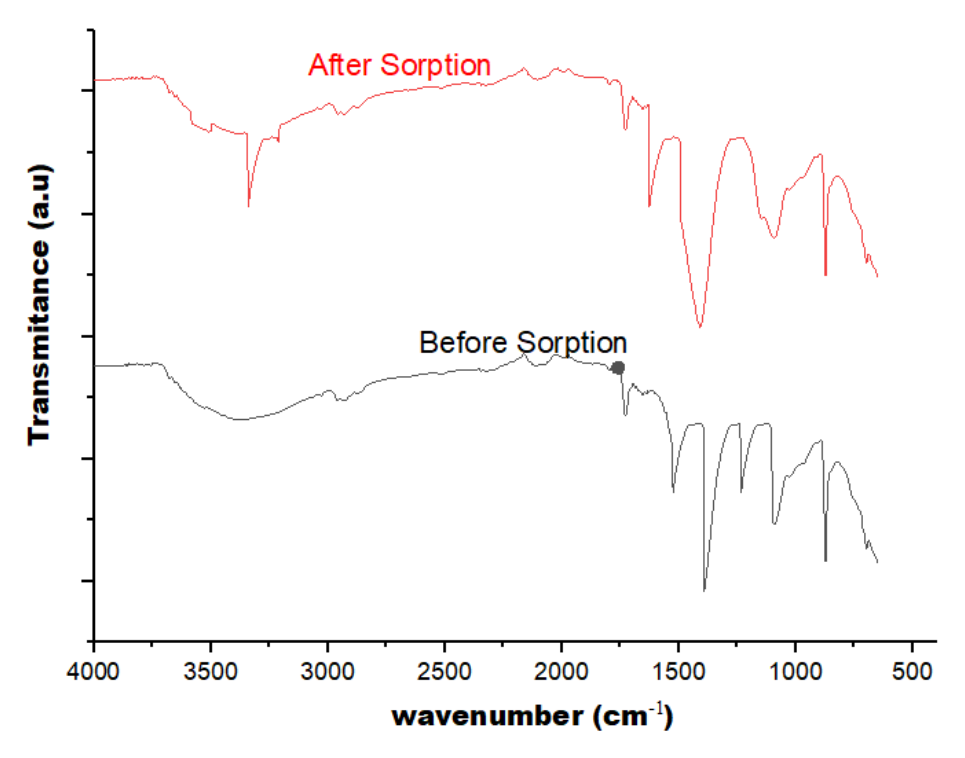


Fig. 13. FTIR graphs of RBPW before and after adsorption of CV

Scanning Electron Microscopic Evaluation of Banana Peel Waste

The scanning electron microscopic (SEM) micrographs labeled as a and b in Fig. 14, represent the surface morphologies of banana peel waste before and after adsorption of CV dye, respectively.

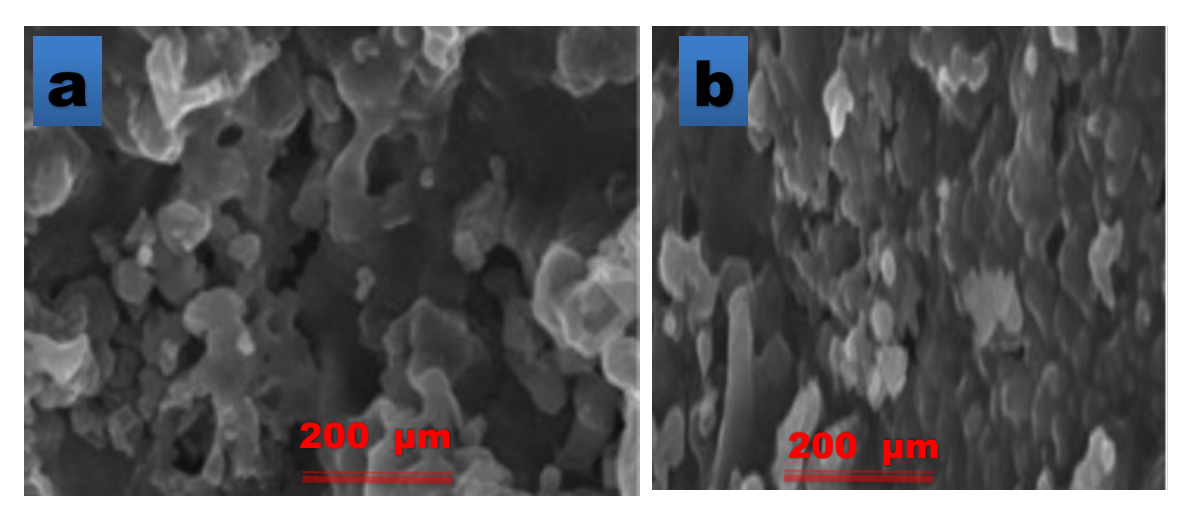


Fig. 14. SEM graphs of RBPW before and after adsorption of CV

Before adsorption of CV, the surface of the banana peel waste appeared porous, rough, and irregular. Some cavities and channels were clearly visible, suggesting a highly

porous structure with a high surface area suitable for capturing dye molecules from aqueous solutions. After adsorption, the surface had undergone a noticeable transformation with the texture becoming more compact and smoother. The porous and irregular morphology observed in SEM images is consistent with the BET results, which indicated that acid treatment increased the surface area and also enhanced pore volume. Similarly, the average pore size increased after acid-treatment, indicating the development of a more mesoporous structure. These quantitative values corroborate the visual evidence from SEM, confirming that acid treatment improved porosity and pore connectivity, which contributed to the higher adsorption capacity of ABPW.

Physicochemical Properties of Raw and Acidified Banana Peel Waste

The physicochemical characteristics of RBPW and ABPW revealed significant improvements following acid treatment, as shown in Table 5. One of the most notable changes was the increase in surface area, from 24.7 m²/g for RBPW to 74.2 m²/g for ABPW. This suggests that acidification effectively removed surface impurities, exposing more active sites for adsorption. As a result, the acidified material offered a much larger surface for pollutant interaction, directly contributing to improved adsorption capacity. Similarly, the pore volume increased from 0.32 cm³/g in RBPW to 0.87 cm³/g in ABPW, further demonstrating the structural benefits of acid treatment, thus providing more or larger pores, allowing better accessibility and retention of dye molecules.

The average pore size also increased slightly from 2.15 nm to 2.86 nm, indicating a shift toward mesoporous structure which could enhance the material's ability to adsorb larger molecules, as mesopores are more favorable for liquid-phase adsorption compared to micropores. A study by Huang *et al.* (2024) noted that treated banana peel powder with 50% H₂SO₄ at 50 °C for 24 h, resulted in an increase in surface area from 0.036 to 0.0507 m²/g, which resulted in impressive Cr(VI) adsorption capacity of 161 mg/g. They further reported that the acid treatment improved porosity, which facilitated pollutant uptake. This is consistent with the changes in surface area and pore volume seen in the current study. A similar study by Channei *et al.* (2025) compared H₂SO₄ and CH₃COOH treatments on banana peel and found that strong acid (H₂SO₄) produced the highest BET surface area (~339 m²/g) and pore volume (~0.059 cm³/g), which is closely related to the increase in surface area and pore volume seen in our study after acidification.

Table 5. Physicochemical Properties of Raw and Acidified Banana Peel Waste

Parameters	RBPW	ABPW
Surface area (m²/g)	24.7	74.2
Pore volume (cm²/g)	0.32	0.87
Average pore size (nm)	2.15	2.86
pH _{ZPC}	4.75	4.14

The observed increase in surface properties after acid treatment can be partly attributed to structural changes caused by the removal of mineral components. In particular, calcium ions bound to carboxyl groups in the lignocellulosic matrix of raw banana peel may act to hold the structure together more tightly. The acid treatment could displace these ions, loosening the structure and exposing more pores, which in turn improves the surface chemistry and adsorption capacity.

CONCLUSIONS

From this study on the use of raw and acidified banana waste peel as adsorbent for crystal violet removal, the following conclusions were made:

- 1. The acidified banana peel achieved higher adsorption capacities in a shorter time frame of 120 min, whereas the raw peel required more time to approach similar capacities and reached equilibrium at 140 min.
- 2. The positive enthalpy changes (+16.4 kJ/mol for raw banana peel waste (RBPW) and +53.5 kJ/mol for acid-treated banana peel waste (ABPW)) indicate the endothermic nature of the adsorption, while positive entropy change (ΔS°) values of +6.79 J/mol·K for RBPW and +14.65 J/mol·K for ABPW suggests increased randomness at the adsorbent–solution interface.
- 3. Fourier transform infrared (FTIR) analysis indicates the presence of –OH, –C=O, –C–O, and aromatic moieties and shows some spectral shifts after sorption process,
- 4. The acid treatment enhanced the surface area, porosity, and surface chemistry of banana peel waste, making ABPW a far more effective adsorbent than its raw counterpart. These improvements make it suitable for a wide range of applications in water and wastewater treatment, particularly for removing cationic contaminants.

ACKNOWLEDGMENTS

The authors express their gratitude to Princess Nourah bint Abdulrahman University Researchers Supporting Project number (PNURSP2025R581), Princess Nourah bint Abdulrahman University, Riyadh, Saudi Arabia.

REFERENCES CITED

- Abdelkhalek, A., Ali, S. S. M., Sheng, Z., Zheng, L., and Hasanin, M. (2022). "Lead removal from aqueous solution by green solid film based on cellulosic fiber extracted from banana tree doped in polyacrylamide," *Fibers Polym.* 23(5), 1171-1181. DOI: 10.1007/s12221-022-4001-y
- Abed, F., Louhab, K., Abai, N., and Babakhouya, N. (2019). "Study of the adsorption of methylene blue by natural materials (olive stone, date pit and their mixture) in fixed bed column," *Alger. J. Environ. Sci. Technol.* 5(2), 947-954.
- Adegoke, K. A., Akinnawo, S. O., Adebusuyi, T. A., Ajala, O. A., Adegoke, R. O., Maxakato, N. W., and Bello, O. S. (2023). "Modified biomass adsorbents for removal of organic pollutants: A review of batch and optimization studies," *Int. J. Environ. Sci. Technol.* 20, 11615-11644. DOI: 10.1007/s13762-023-04872-2
- Ahmad, R., and Ansari, K. (2020). "Polyacrylamide-grafted *Actinidia deliciosa* peels powder (PGADP) for the sequestration of crystal violet dye: Isotherms, kinetics and thermodynamic studies," *Appl. Water Sci.* 10, article 195. DOI: 10.1007/S13201-020-01263-7.

- Ahmed, U., Sundholm, D., and Johansson, M. P. (2024). "The effect of hydrogen bonding on the π depletion and the π - π stacking interaction," *Phys. Chem. Chem. Phys.* 26, 27431-27438. DOI. 10.1039/D4cp02889A
- Akpomie, K. G., and Conradie, J. (2020). "Banana peel as a biosorbent for the decontamination of water pollutants. A review," *Environ. Chem. Lett.* 18, 1085-1112. DOI: 10.1007/s10311-020-00995-x
- Akter, M., Rahman, F. B. A., Abedin, M. Z., and Kabir, S. M. F. (2021). "Adsorption characteristics of banana peel in the removal of dyes from textile effluent," *Textiles* 1(2), 361-375. DOI: 10.3390/textiles1020018
- Aljeboree, A. M., Al-Baitai, A. Y., Abdalhadi, S. M., and Alkaim, A. F. (2021). "Investigation study of removing methyl violet dye from aqueous solutions using corn-cob as a source of activated carbon," *Egypt. J. Chem.* 64(6), 2873-2878. DOI: 10.21608/ejchem.2021.55274.3159
- Azhar-ul-Haq, M., Javed, T., Abid, M., Masood, H. T., and Muslim, N. (2022). "Adsorptive removal of hazardous crystal violet dye onto banana peel powder: equilibrium, kinetic and thermodynamic studies," *J. Disper. Sci. Technol.* 1–16. DOI: 10.1080/01932691.2022.2158851.
- Baharim, N. H., Sjahrir, F., Mohd, T. R., Idris, N., and Tuan, D. T. A. (2023). "Removal of crystal violet from aqueous solution using post-treated activation biochar derived from banana pseudo stem," *Chem. Eng. Transac.* 98, 45-50. DOI: 10.3303/CET2398008
- Cao, S., Zhu, R., Wu, D., Su, H., Liu, Z., and Chen, Z. (2024). "How hydrogen bonding and π-π interactions synergistically facilitate mephedrone adsorption by bio-sorbent: An in-depth microscopic scale interpretation," *Environ Pollut*. 342, article 123044. DOI: 10.1016/j.envpol.2023.123044.
- Channei, D., Jannoey, P., Thammaacheep, P., Khanitchaidecha, W., and Nakaruk, A. (2025). "From waste to value: Banana-peel-derived adsorbents for efficient removal of polar compounds from used palm oil," *Applied Sciences* 15(4), article 2205. DOI: 10.3390/app15042205
- Cheng, X., Duan, C., Yang, P., Pi, Y., Qi, H., Sun, Z., and Chen, S. (2023). "Effective adsorption of crystal violet onto magnetic nanoparticles decorated bacteria: Kinetic and site energy distribution analysis," *Process Saf. Environ. Prot.* 173, 837-846. DOI: 10.1016/J.PSEP.2023.03.035
- Dada, A., Olalekan, A., Olatunya, A., and Dada, O. (2012). "Langmuir, Freundlich, Temkin and Dubinin-Radushkevich isotherms studies of equilibrium sorption of Zn²⁺ unto phosphoric acid modified rice husk," *J. Appl. Chem.* 3(1), 38-45. DOI. 10.9790/5736-0313845
- Edet, U. A., and Ifelebuegu, A. O. (2020). "Kinetics, isotherms, and thermodynamic modeling of the adsorption of phosphates from model wastewater using recycled brick waste," *Processes* 8(6), article 665. DOI: 10.3390/pr8060665
- El-Rayyes, A., Arogundade, I., Ogundiran, A. A., Hefnawy, M., Ofudje, E. A., El Gamal, A., Albedair, L. A., and Alsuhaibani, A. M. (2025). "Hot water-treated cow waste use as an efficient adsorbent for cresol red dye and chromium VI removal from aqueous solutions," *BioResources* 20(2), 3252-3285. DOI: 10.15376/biores.20.2.3252-3285
- Enniya, I., Rghioui, L., and Jourani, A. (2017). "Adsorption of hexavalent chromium in aqueous solution on activated carbon prepared from apple peels," *Sustain. Chem. Pharm.* 7, 9-16. DOI: 10.1016/j.scp.2017.11.003

- Gemici, B. T. (2023). "Crystal violet adsorption onto modified biosorbent prepared from agricultural waste: Kinetics, isotherm and thermodynamic studies," *Chem. Eng. Comm.* 211(4), 582-591. DOI: 10.1080/00986445.2023.2266677
- Girish, C.R. (2025). "Determination of thermodynamic parameters in adsorption studies: A review," *Chem. Pap.* DOI: 10.1007/s11696-025-04218-x
- Guo, S., Zou, Z., Chen, Y., Long, X., Liu, M., Li, X., Tan, J., and Chen, R. (2023). "Synergistic effect of hydrogen bonding and π - π interaction for enhanced adsorption of rhodamine B from water using corn straw biochar," *Environ Pollut.* 1, 320, article 121060. DOI: 10.1016/j.envpol.2023.121060.
- Homagai, P. L., Poudel, R., Poudel, S., and Bhattarai, A. (2022). "Adsorption and removal of crystal violet dye from aqueous solution by modified rice husk," *Heliyon* 8(4), article e09261. DOI: 10.1016/J.HELIYON.2022.E09261.
- Huang, Z., Campbell, R., and Mangwandi, C. (2024). "Kinetics and thermodynamics study on removal of Cr(VI) from aqueous solutions using acid-modified banana peel (ABP) adsorbents" *Molecules* 29(5), article 990. DOI: 10.3390/molecules29050990.
- Huang, Y., Niu, H., Jin, L., Jiao, L., Johnson, D., Tian, H., Sarina, S., Zhu, H., and Fang, Y, (2023). "Selective adsorption of crystal violet via hydrogen bonded water bridges by InvO₄," available at
 - SSRN: https://ssrn.com/abstract=4414836 or http://dx.doi.org/10.2139/ssrn.4414836
- Hubbe, M. A., Azizian, S., and Douven, S. (2019). "Implications of apparent pseudo-second-order adsorption kinetics onto cellulosic materials. A review," *BioResources* 14(3), 7582-7626. DOI: 10.15376/biores.14.3.7582-7626
- Jahin, H. S., Khedr, A. I., and Ghannam, H. E. (2024). "Banana peels as a green bioadsorbent for removing metals ions from wastewater," *Discov. Water* 4(36). DOI: 10.1007/s43832-024-00080-2.
- Jia, Z., Li, Z., Ni, T., and Li, S. (2017). "Adsorption of low-cost absorption materials based on biomass (*Cortaderia selloana* flower spikes) for dye removal: Kinetics, isotherms and thermodynamic studies," *J. Molecular Liquids* 285-292. DOI: 10.1016/j.molliq.2016.12.059.
- Liu, L., Fan, S., and Li, Y. (2018). "Removal behavior of methylene blue from aqueous solution by tea waste: kinetics, isotherms and mechanism," *Int. J. Environ. Res. Public Health* 15(7), article 1321. DOI: 10.3390/ijerph15071321
- Mittal, H. A., Morajkar, P. P., and Alhassan, S. M. (2021). "Graphene oxide crosslinked hydrogel nanocomposites of xanthan gum for the adsorption of crystal violet dye," *J. Mol. Lig.* 323, article 115034. DOI: 10.1016/j.molliq.2020.115034
- Muhammad, M. K., Amina, K., Haq, N. B., Zahid, M., Alissa, S. A., El-Badry, Y. A., Hussein, E. E., and Iqbal, M. (2021). "Composite of polypyrrole with sugarcane bagasse cellulosic biomass and adsorption efficiency for 2,4-dicholrophonxy acetic acid in column mode," *J. Mat. Res. and Technol.* 2016-2025. DOI: 10.1016/j.jmrt.2021.09.028
- Naseem, K., Ahmad, K., Anwar, A., Farooqi, Z. H., Najeeb, J., Iftikhar, M. A., Hassan, W., Ul, B. A., Haider, S., and Akhtar, M. S. (2023). "*Raphanus caudatus* biomass powder as potential adsorbent for the removal of crystal violet and Rhodamine B dye from wastewater," *Z. Phys. Chem.* 237, 1863-1883. DOI: 10.1515/zpch-2023-0259
- Ngueagni, P. T., Hefnawy, M., Ofudje, E. A., El Gamal, A., Akande, J. A., and Emran, T. B. (2025). "Cellulose-based adsorbent of animal waste for the adsorption of lead and phenol," *BioResources* 20(2), 3923-3952. DOI: 10.15376/biores.20.2.3923-3952

- Ofudje, E. A., Adeogun, I. A., Idowu, M. A., Kareem, S. O., and Ndukwe, N. A. (2020). "Simultaneous removals of cadmium(II) ions and reactive yellow 4 dye from aqueous solution by bone meal-derived apatite: Kinetics, equilibrium and thermodynamic evaluations," *J. Anal. Sci. Technol.* 11, 7. DOI: 10.1186/s40543-020-0206-0
- Ofudje, E. A., Al-Ahmary, K. M., Alzahrani, E. A., Ud Din, S., and Al-Otaibi, J. S. (2024). "Sugarcane peel ash as a sorbent for methylene blue," *BioResources* 19(4), 9191-9219. DOI: 10.15376/biores.19.4.9191-9219
- Ofudje, E. A., Sodiya, E. F., Akinwunmi, F., Ogundiranc, A. A., Oladeji, O. B., and Osideko, O. A. (2022). "Eggshell derived calcium oxide nanoparticles for toluidine blue removal," *Desali. Water Treat.* 247, 294-308. DOI: 10.5004/dwt.2022.28079
- Ogundiran, A. A., Ogundiran, O. O., Adejoke, B., El Gamal, A., Emran, T. B., and Hefnawy, M. (2025). "Sustainable wastewater treatment: Raw and activated cow dung for the sorption of methylene blue dye," *BioResources* 20(3), 6815-6836. DOI: 10.15376/biores.20.3.6815-6836
- Onuk, E. B., and Isik, B. (2025). "Adsorptive removal of toxic methylene blue and crystal violet dyes from aqueous solutions using *Prunus spinosa*: Isotherm, kinetic, thermodynamic, and error analysis," *Biomass Conv. Bioref.* DOI: 10.1007/s13399-025-06519-3
- Pagalan Jr., E., Sebron, M., Gomez, S., Salva, S. J., Ampusta, R., Macarayo, A. J., Joyno, C., Ido, A., and Arazo, R. (2020). "Activated carbon from spent coffee grounds as an adsorbent for treatment of water contaminated by aniline yellow dye," *Industrial Crops and Products* 145, article 111953. DOI:10.1016/j.indcrop.2019.111953
- Palle, K., Vunguturi, S., Rao, K. S., Gayatri, S. N., Babu, P. R., Ali, M., and Kola, R. (2022). "Comparative study of adsorption isotherms on activated carbons synthesized from rice husk towards carbon dioxide adsorption," *Chem. Pap.* 76, 7525-7534. DOI: 10.1007/s11696-022-02371-1
- Parlayıcı, Ş., and Baran, Y. (2025). "A novel alginate/fruit waste/Fe₃O₄ hydrogel biobeads for highly efficient removal of methylene blue from aqueous solution," *Polym. Bull.* DOI: 10.1007/s00289-025-05814-3
- Pashaei-Fakhri, S., Peighambardoust, S. J., Foroutan, R., Arsalani, N., and Ramavandi, B. (2021). "Crystal violet dye sorption over acrylamide/graphene oxide bonded sodium alginate nanocomposite hydrogel," *Chemosphere* 270, article 129419. DOI: 10.1016/j.chemosphere.2020.129419
- Popoola, L. T., Yusuff, A. S., Taura, U., Oladokun, D. I., Adeyi, A. A. and Aderibigbe, T. A. (2024). "Wastewater treatment from a typical multisystem hospital using chemically modified banana peels: Taguchi parametric optimization and characterization," *Appl. Water Sci.* 14, article 112. DOI:10.1007/s13201-024-02173-8
- Rehali, H., Elbar, D., Ghiaba, L., and Bounafi, K. (2021). "Elimination of nickel (II) in water with different activated carbons (dates nut, peach nuts and apricot kernels)," *Dig J Nanomater Biostructures* 16(1), 109-118. DOI. 10.152551/djnb.2021.161.109
- Sahmoune, M. N., Moussa, A., and Mohamed, T. (2024). "Understanding the rate-limiting step adsorption kinetics onto biomaterials for mechanism adsorption control," *Progress in Reaction Kinetics and Mechanism* 49, 1-26. DOI: 10.1177/14686783241226858
- Sen, N., Shefa, N. R., Reza, K., Sk MdAli, Z. S., and Md. Wasikur, R. (2024). "Adsorption of crystal violet dye from synthetic wastewater by ball-milled royal palm leaf sheath," *Sci. Rep.* 14, article 5349. DOI: 10.1038/s41598-024-52395-8

- Shridhar, K. J., and Sanjaykumar, R. T. (2022). "Adsorption isotherm study of crystal violet dye onto biochar prepared from agricultural waste," *Oriental Journal of Chemistry* 38(2), 475-481. DOI.10.13005/ojc/380234
- Silviyanti, I., Supraptiah, E., Niati, S. M., Hajar, I., Ningsih, A. S., and Amalda, F. N. (2025). "Effectiveness of Kepok banana (*Musa paradisiaca*) bread-based adsorbent for Fe(III) removal using HCl activation: Freundlich and Langmuir isotherm models," *Chempublish Journal* 9(1), 130-140. DOI: 10.22437/chp.v9i1.44926
- Thomas, B., Shilpa, E. P., and Alexander, L. K. (2021). "Role of functional groups and morphology on the pH dependent adsorption of a cationic dye using banana peel, orange peel, and neem leaf bio–adsorbents," *Emerg Mater Res* 4(5), 1479-1487. DOI: 10.1007/s42247-021-00237-y
- Wang, R.-F., Deng, L.-G., Li, K., Fan, X.-J., Li, W., and Lu, H.-Q. (2020). "Fabrication and characterization of sugarcane bagasse calcium carbonate composite for the efficient removal of crystal violet dye from wastewater," *Ceramics International* 27484-27492. DOI: 10.1016/j.ceramint.2020.07.237.
- Yang, X., Wan, Y., Zheng, Y., He, F., Yu, Z., Huang, J., Wang, H., Ok, Y., S., Jiang, Y., Gao, B. (2019). "Surface functional groups of carbon-based adsorbents and their roles in the removal of heavy metals from aqueous solutions: A critical review," *Chem. Eng. J.* 366, 608-621. DOI: 10.1016/j.cej.2019.02.119
- Yuan, L., and Jiang, W. (2021). "Porous cellulose triacetate particles prepared from recycled corrugated cases for adsorption of crystal violet," *J. Appl. Polym. Sci.* 138, article 50981, DOI: 10.1002/app.50981

Article submitted: July 21, 2025; Peer review completed: August 24, 2025; Revised version received: August 26, 2024; Accepted: October 13, 2025; Published: October 23, 2025.

DOI: 10.15376/biores.20.4.10640-10664